Magnetism and electronic transport in (Cu,Ni)2MnSn Heusler alloys under ambient and elevated pressures

S.K. Bose, Physics Department, Brock University, St. Catharines, Ontario L2S 3A1 Canada
J. Kudrnovský and V. Drchal, Institute of Physics, Czech Academy of Sciences, Prague 8, Czech Republic

Introduction

Heusler alloys are materials with interesting physical properties and significant potential technological applications (magnetic shape memory, magnetocaloric effects, and spintronics). Structurally, most Heusler alloys crystallize in two different cubic phases, having either $L2_1$ or C_{1b} symmetry. An important feature of Heusler alloys is the presence of chemical or substitutional disorder. Examples are the chemical disorder due to non-stoichiometry or a native chemical disorder which exists even in 'ideal' ordered alloys. The complex quaternary alloys like the semi-Heusler (Ni,Cu)MnSb alloys are another example. Here we present results of our *first-principles* density-functional studies of magnetic, thermodynamical, and transport properties of full quaternary $(Cu,Ni)_2MnSn$ Heusler alloys, some of which have appeared in our recent publication [1]. Our resistivity calculation includes the effect of both chemical disorder between Cu and Ni atoms and the spin-disorder due to finite temperature effects.

Method

(a) electronic structure

The electronic structure calculations were carried out using the TB-LMTO method [2] in which the effect of disorder is included via the coherent potential approximation [3]. We use the exchange-correlation potential, based on spin density functional theory, given by Vosko, Wilk, Nusair [4] and employ the experimental lattice constants [5]. Electronic properties, such as the density of states, are calculated using standard band structure methods.

(b) exchange interaction

The exchange interactions among Mn atoms, influenced by the disorder among Cu and Ni atoms, are obtained via the mapping of the total (band) energy onto a Heisenberg spin-Hamiltonian form suggested by Liechtenstein [6]:

$$H_{\rm eff} = -\sum_{i,j} J_{ij}\, \mathbf{e}_i \cdot \mathbf{e}_j \,, \qquad (1)$$

where i, j are site indices, $\mathbf{e}_i$ is the unit vector pointing along the direction of the local magnetic moment at site i, and J_{ij} is the exchange integral between sites i and j. Using Green's function and multiple-scattering formalism, the exchange integral in Eq.(1) can be shown to be given by

$$J_{ij} = \frac{1}{4\pi} \lim_{\epsilon\to 0^+} Im \int tr_L \left[\Delta_i(z) g_{ij}^{\uparrow}(z) \Delta_j(z) g_{ji}^{\downarrow}\right] dz \,, \qquad (2)$$

where $z = E + i\epsilon$ represents the complex energy variable, $L = (l, m)$, and $\Delta_i(z) = P_i^{\uparrow}(z) - P_i^{\downarrow}(z)$, representing the difference in the potential functions for the up and down spin electrons at site 'i'. In the present work $g_{ij}^{\sigma}(z)(\sigma = \uparrow, \downarrow)$ represents the matrix elements of the Green's function of the medium for the up and down spin electrons. The exchange integrals in Eq. (2) are energy dependent and their physical values appropriate for the system at hand is obtained by setting this energy equal to the Fermi energy E_F: $J_{ij} = J_{ij}(E)|_{E=E_F}$. The exchange integrals, by construction, contain the atom magnetic moments, their positive (negative) values being indicative of ferromagnetic (antiferromagnetic) coupling. Calculated exchange integrals are used to estimate the spin-stiffness and the Curie temperature T_c using both mean field and random phase approximations (MFA and RPA). One can obtain the Curie temperature T_c in mean field approximation (MFA) from

$$k_B\, T_c^{\rm MFA} = \frac{2}{3} \sum_{i\neq 0} J_{0i}^{\rm Cr,Cr} \,, \qquad (3)$$

where the sum extends over all the neighboring shells. Random phase approximation (RPA) provides an improved estimate of T_c given by

$$(k_B\, T_c^{\rm RPA})^{-1} = \frac{3}{2}\frac{1}{N} \sum_{\mathbf{q}} [J^{\rm Cr,Cr}(\mathbf{0}) - J^{\rm Cr,Cr}(\mathbf{q})]^{-1} \,. \qquad (4)$$

Here N denotes the order of the translational group applied and $J^{\rm Cr,Cr}(\mathbf{q})$ is the lattice Fourier transform of the real-space exchange integrals $J_{ij}^{\rm Cr,Cr}$.

(c) electronic transport properties

The residual resistivity is determined by the linear-response theory as formulated in the framework of the TB-LMTO-CPA approach using the Kubo-Greenwood (K-G) formula [7, 8]. Within the K-G formalism, transport properties, such as conductance or conductivity at the energy E: $\sigma(E)$, can be expressed in the form

$$\sigma(E) \propto Tr\left\{\delta(E-H) J \delta(E-H) J\right\} \,, \qquad (5)$$

where J is the velocity or current operator. The physical conductivity is obtained by setting $E = E_F$. The velocity/current operator can be related, via the Heisenberg equation of motion, to the commutator of the Hamiltonian H and the position operator x (with $e = \hbar = 1$):

$$J = -i[x, H] \,. \qquad (6)$$

The Dirac delta functions appearing in Eq.(5) can be related to the imaginary part of the Green's function

$G(E-H)$. The representation of the Green's function and the evaluation of the matrix elements of J in the TB-LMTO basis has been discussed in details in Refs. [7, 8].

The spin disorder [9] is described in the framework of the disordered local moment (DLM) picture [10]. The DLM model treats the paramagnetic state as one in which nonzero local moments point up or down with equal probability for the same atom. This spin disorder is akin to 'substitutional' disorder in a binary alloy and can be treated via CPA [3]. A modification of this is the uncompensated DLM model where the probabilities of up and down spins are modified to give a net magnetic moment to each atom, thus representing a FM state. Resistivity due to this spin disorder can be treated in the same way as the residual resistivity using the K-G formalism.

(d) spin-wave stiffness

We have also computed the spin-wave stiffness constant D which describes the long wavelength (low wave vector q) magnon dispersion of the system. For cubic systems the low q dispersion is spherically symmetric: $E(\mathbf{q}) = Dq^2$, where $q = |\mathbf{q}|$ and $E(\mathbf{q})$ is the spin-wave energy, realted to the exchange parameters J_{ij} by

$$E(\mathbf{q}) = \frac{4\mu_B}{M} \sum_{j \neq 0} J_{0j} \left(1 - \exp[i\mathbf{q} \cdot \mathbf{R}_{0j}]\right) \ , \qquad (7)$$

where $\mathbf{R}_{0j} = \mathbf{R}_0 - \mathbf{R}_j$ denote lattice vectors in real space, and $\mathbf{q}$ is a vector in the corresponding Brillouin zone. M is the magnetic moment per atom in μ_B, the Bohr magneton. For lattices with inversion symmetry and low q, Eq. (7) yields

$$D = \frac{2\mu_B}{3M} \sum_{j \neq 0} J_{0j} R_{0j}^2 \ , \qquad (8)$$

The practical difficulties associated with evaluating D from the slow convergence of the above sum has been discussed in detail by Pajda *et al.* [11]. Often a solution is to use a damping factor η and compute D from the limit $D = \lim_{\eta \to 0} D(\eta)$, where

$$D(\eta) = \lim_{R_{max} \to \infty} \frac{2\mu_B}{3M} \sum_{0 < R_{0j} \leq R_{max}} J_{0j} R0j^2 \exp(-\eta R_{0j}/a) \ , \qquad (9)$$

a being the lattice parameter.

Results

Fig. 1 shows the calculated local densities of states (LDOSs) of nonmagnetic X_2MnSn (X=Cu, Ni, Pd) alloys. Several conclusions follow immediately: (i) all DOSs have a pronounced peak at the Fermi energy (E_F), indicating instability against formation of the ferromagnetic state (Stoner criterion). (ii) The dominant contribution to the peaks is from the Mn-LDOS, which suggests that the magnetism is primarily due to the Mn-sublattice. (iii) The height of Mn-LDOS(E_F) (which is $\sim$ total DOS(E_F)) is approximately the same in all cases, indicating similar magnetic moments for all these compounds. (iv)The increasing bandwidth of the d-states dominating local X-LDOS as we move from Cu to Ni. This is indicative of decreasing localization (increasing itinerancy) of the d-electrons, resulting in decreasing T_c in the same order, according to the model proposed by Stearns [12]. (v) The Cu- and Ni-bands are well separated in energy resulting in a strong diagonal disorder. The difference in their d-bandwidths (off-diagonal disorder) is smaller than the separation of the centers of the d-bands. This implies that off-diagonal disorder is weaker than the diagonal disorder, the latter being the more dominant factor for transport properties such as resistivity.

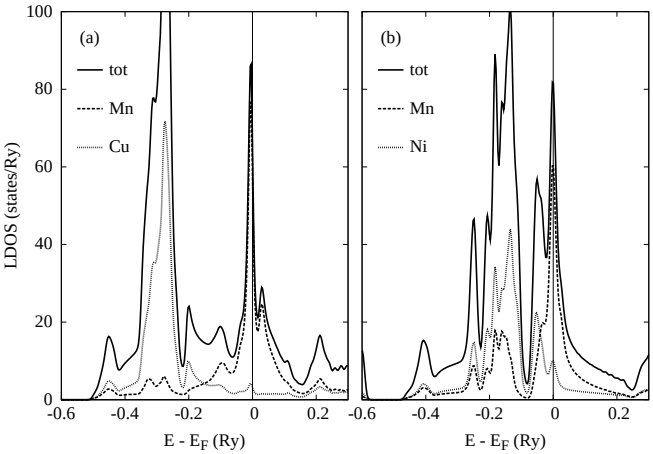

Figure 1: *Total and component resolved densities of states, per formula unit and spin, for nonmagnetic Heusler alloys: (a) ordered Cu_2MnSn, (b) ordered Ni_2MnSn.*

The spin-polarized LDOS for Ni_2MnSn, $(Ni_{50},Cu_{50})_2MnSn$, and Cu_2MnSn are shown in Fig. 2. The following conclusions can be drawn: (i) Spin-polarized Cu-LDOSs in Cu_2MnSn are almost identical, indicating practically no polarization, while some small polarization is seen for corresponding Ni-LDOS in Ni_2MnSn. Similar conclusions are also valid for Cu- and Ni-LDOSs for the equiconcentration case (Fig. 2b). (ii) The total LDOS is smoothed by strong level disorder in the equiconcentration alloy. (iii) Due to large level splitting (large local magnetic moment) the minority Mn-bands in all cases hybridize very little with the Ni- or Cu-bands. On the contrary, such hybridization, compared to the nonmagnetic case, is strong for the majority bands even for Cu_2MnSn. (iv) The majority and minority states at the Fermi energy behave differently (corresponding DOSs have different curvature). This results in different Fermi surface geometry for these bands (see e.g. Ref. [13]).

Concentration dependence of the magnetic moment in this alloy system is discussed and shown in detail in Ref. [1]. There is an overall good agreement between calculated and measured [5] average moments, which are essentially concentration-independent and have val-

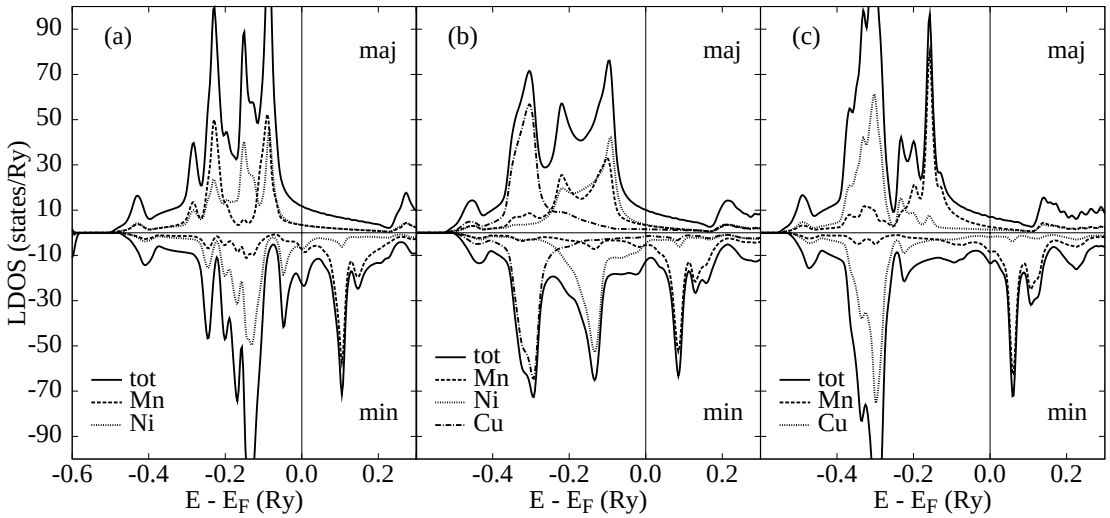

Figure 2: *Total and component resolved densities of states, per formula unit and spin, for ferromagnetic Heusler alloys: (a) ordered Ni_2MnSn, (b) disordered $(Ni_{50},Cu_{50})_2MnSn$, and (c) ordered Cu_2MnSn.*

ues around 4 μ_B. The contribution from Mn-atom dominates, with the Ni-moments being smaller than 0.2 μ_B and other moments being negligible. The large intra-atomic exchange splitting of Mn atoms and the small hybridization of minority Mn-d orbitals with the X-atom orbitals lead to the full occupation of majority Mn-d orbitals, to negligible spin polarization of X- and Sn-atom orbitals, and to composition-independent occupation of minority Mn-d orbitals. These features result in the nearly constant Mn-moment and the total alloy magnetization.

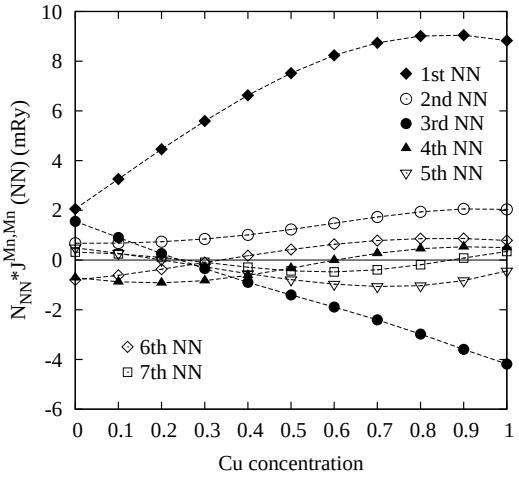

Figure 3: *The first 7 exchange interactions (multiplied by their degeneracies) as a function of Cu- concentration.*

Exchange integrals, derived form the DLM reference state and multiplied by degeneracy factors, are shown in Fig. 3. The resulting concentration dependence is quite complex, with the first three exchange integrals being dominant. While the first two are ferromagnetic and increase with the Cu-content, the third one decreases almost linearly with Cu-concentration, and changes its sign at about 20% of Cu, giving a hockey-stick like shape to the non-monotonic variation of the Curie temperature with concentration (see Fig. 4). T_cs calculated in the framework of the RPA are in good agreement with the measured values [14]. We find that the MFA overestimates T_c and fails to reproduce correctly (even in a qualitative sense) the variation of T_c with concentration.

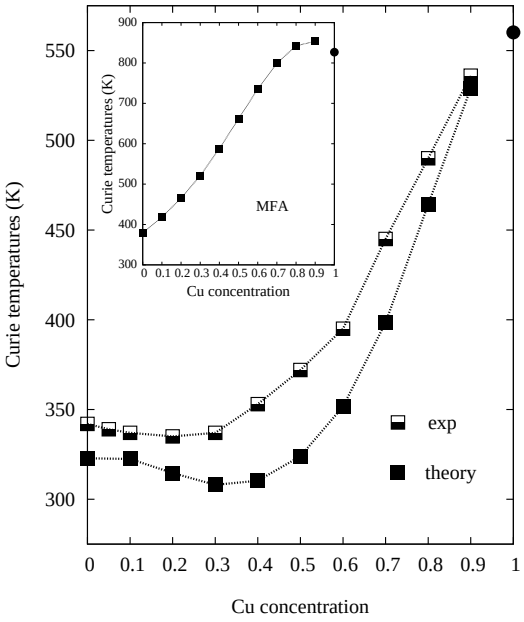

Figure 4: *Calculated (RPA) and experimental Curie temperatures as a function of Cu-concentration. The MFA results are shown in the inset.*

We also estimate the spin-stiffness constant D for Ni_2MnSn from exchange constants using the ferromag-

netic reference state and the limiting procedure involving the exponential damping factor as shown by Eq. (9) (see [11] for details). The calculated and experimental [15] values of D for Ni_2MnSn alloy are 160 $\pm$25 and 150 $\pm$10 meV.Å^2, respectively.

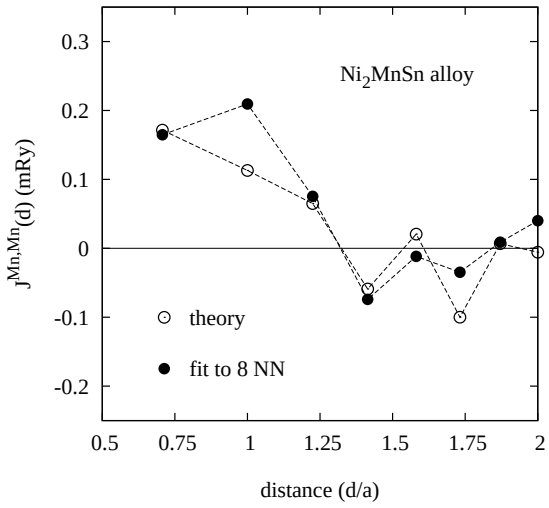

Figure 5: *Comparison of calculated exchange integrals (present paper, theory) with those obtained from the fit to neutron spin-wave scattering experiment (Table I of Ref. [15], 8 NN fit).*

In Fig. 5 we compare the calculated exchange integrals with those extracted from the measured inelastic neutron spin-wave scattering data by Noda and Ishikawa [15]. These authors use upto 8 nearest neighbour (NN) fit to extract the exchange interaction for various neighbour shells. Fig. 5 compares our calculated values with their 8 NN fit. The general agreement between the calculated results and the extracted values from the fit appears to be good. Noda and Ishikawa [15] have presented results for 4-,6-,7-, and 8-neighbour shells fit to their neutron scattering data. It should be noted that calculated exchange integrals are not limited by the distance 2 a (8 NN) as the fitted ones. In fact, saturation of results with respect to the number of shells is not achieved for 8 NN interactions. It is also clear from Table I of Ref. [15] that the fitted values can change significantly depending on the number of shells of neighbours used for a fit. For example, in case of Ni_2MnSn the 2nd neighbor interaction is larger than that of the 1st neighbor for the 8 NN fit, and smaller for the 6 NN fit.

In magnetic alloys there are three contributions to the resistivity: the temperature (T)-independent residual resistivity due to the alloy disorder and other defects, and two T-dependent terms: one due to electron-phonon scattering and the other due electron-magnon (spin disorder) scattering. In Fig. 6 we show the concentration dependence of the resistivity of $Ni_{1-x}Cu_x)_2MnSn$ alloy due to spin-disorder evaluated for temperatures $T \geq T_c$. For $T \geq T_c$, where the magnetic state is paramagnetic, i.e. the local moments are completely random with zero net magnetic moment, the spin-disorder resistivity is T-independent and we calculate this using the DLM model and the G-K formula. The readers should note that the resistivity shown in Fig. 6 (main frame) accounts for only the spin-disorder and does not include the (T-dependent) contribution from electron-phonon scattering. The inset of Fig. 6 shows the concentration-dependence of the residual resistivity in $(Ni_{1-x},Cu_x)_2MnSn$, which seems to follow the weak-scattering Nordheim rule: $\rho \propto x(1-x)$, being maximum at the 50-50 composition.

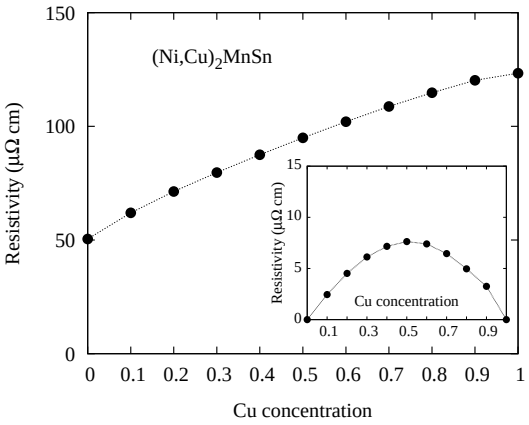

Figure 6: *The concentration-dependence of the spin-disorder resistivity (T-independent) valid for temperatures $T \geq T_c$. The inset shows residual resistivities of $(Ni_{1-x},Cu_x)_2MnSn$ alloys evaluated for the ferromagnetic ground state at zero temperature.*

To capture the T-dependence of the spin-disorder resistivity below T_c one could use the uncompensated DLM model. The results from using such a model has recently been discussed by us [1] (see Fig.12 of this reference). Here we present results based on a simpler semi-empirical approach.

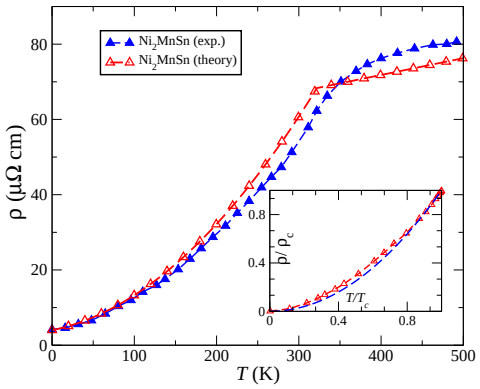

Figure 7: *(Color online) Calculated and experimental T-dependent resistivities of Ni_2MnSn. Validity of a simple model for the effect of spin-disorder on resistivity (see text) is illustrated in the inset.*

In Fig. 7 we display theoretically calculated resistivity of Ni_2MnSn as a function of temperature assuming the

form [16] $\rho(T) = \rho_0 + AT + BT^2$. The quadratic term is based on a theory of the spin-disorder resistivity given by Kasuya [9], the linear one is the phonon contribution (which is valid with the exception of very low temperatures), and ρ_0 is the value of the residual resistivity at T=0 K, which is due to all the defects present in the sample. While constants ρ_0 and A are taken from the experiment [17], constant B is calculated from the expression $B = \rho_c/(T_c)^2$. Here ρ_c denotes the resistivity evaluated at the Curie temperature T_c. We identify ρ_c with the resistivity in the paramagnetic (DLM) state and T_c as calculated above. This approximation is valid if the spin-spin correlation function is small at T_c, a reasonable assumption for a number of transition metals and their alloys, including the Heusler alloys. We demonstrate the validity of this simple model in the inset of Fig. 7, a plot of the reduced resistivity ρ/ρ_c vs reduced temperature T/T_c. The assumed quadratic dependence (dashed line) is supported very well by the experiment for the extracted spin-disorder part (symbols). We obtain very good quantitative agreement between the measured and calculated temperature-dependent resistivity. The theoretical estimate B= 4.7×10^{-4}$\mu\Omega$ cm K^{-2} compares reasonably well with the experiment (3.94×10^{-4}$\mu\Omega$ cm K^{-2}). We refer the reader to our recent paper [1] for further details and for results involving other related systems.

There exists a number of experimental studies of the variation of the Curie temperature (T_c) under pressure for transition-metal elements and alloys [18, 19] as well as some Heusler alloys including [20] Ni_2MnSn, [21, 22] Pd_2MnSn and some others [22]. However, the corresponding experimental studies of the pressure-dependence of the resistivity are rare: one example of such a study is the work by Austin and Mishra [22].

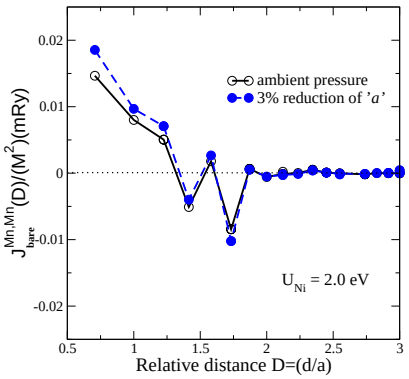

Figure 8: *The bare exchange interactions $J^{Mn,MN}_{bare}$ defined as $J^{Mn,MN}/(M^{MN})^2$, where $J^{Mn,MN}$ is the conventional exchange integral as obtained from the mapping of the energy into the Heisenberg Hamiltonian and given by Eq. (2), and M^{Mn} denotes the absolute value of the local magnetic moment of the Mn-atoms in the DLM state. The cases of ambient pressure and the pressure corresponding to the 3% reduction of the lattice parameter are shown for the Ni_2MnSn Heusler alloy.*

In Fig. 8 we show the changes in the bare exchange interaction due to lattice compression in Ni_2MnSn Heusler alloy. The bare exchange interaction J^{bare}_{ij} is defined as $J^{bare}_{ij} = J_{ij}/(M_iM_j)$, where M_i denotes the size of the local magnetic moment of Mn atom at site i. This definition is motivated by the presence of the exchange splittings $\Delta_i(z)$ in Eq. (2) which are roughly proportional to the moment magnitudes M_i. With increasing pressure, local moments usually decrease in magnitude - a typical result of band broadening. On the other hand, the bare exchange interaction increases. This is due to the fact the matrix elements of the exchange potential between the wavefunctions at the Fermi energy is inversely proportional to the volume of the system, as the wavefunctions are normalized within the system volume. The resultant change in T_c is thus a combination of these two competing factors. Fig. 8 clearly shows this increase for the first five neighbour interactions.

Results for the pressure-dependence of T_c in $(Ni,Cu)_2MnSn$ alloy over a set of pressures realized by a linear reduction of the alloy lattice constant from the ambient value up to 3% are shown in Fig. 9.

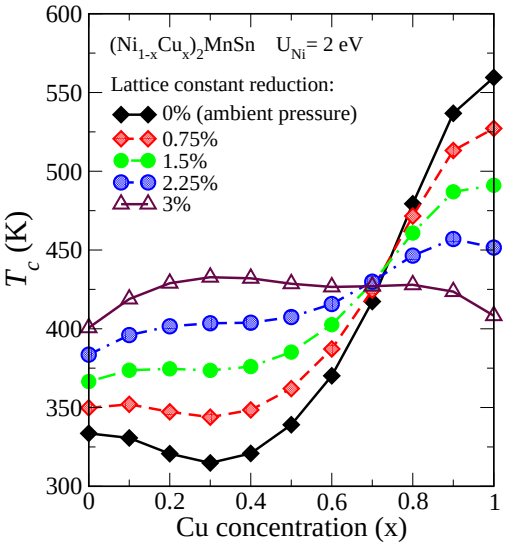

Figure 9: *The concentration dependence of Curie temperatures (RPA) for $(Ni_{1-x},Cu_x)_2MnSn$ alloys for ambient pressure and for set of pressures corresponding to indicated reductions of the alloy lattice constant. Model assumes electron correlations on Ni-sites treated in the framework of the LSDA+U method.*

The results for ambient pressure are slightly improved for the present LSDA+U model as compared to the LSDA results of our previous study, [1] but the general trend is the same. Specifically, we observe two concentration regions, the first one for $x \leq 0.4$ in which T_c is essentially constant with shallow minima and that for $x > 0.4$ where T_c increases monotonically with compo-

sition. Under increasing pressure the behavior in the first concentration region remains unchanged, but there is a gradual reduction of the slope in the other concentration region (the Cu-rich end). Such a development is clearly related to an opposite trend in the pressure-dependence of Cu_2MnSn, namely a reduction of T_c with pressure. The crossover from the positive derivative of the pressure-dependence of T_c to the negative one takes place around x=0.7. Thus, for the pressure corresponding to a 3% reduction of the lattice constant we predict only a weak dependence of T_c on the alloy composition.

The temperature-dependence of the spin-disorder resistivity, calculated in the same way as described for Fig. 7, at ambient pressure and pressure corresponding to 3% reduction of the lattice parameter is shown in Fig. 10. We find that the resistivity at the Curie temperature increases with pressure, but this result is mostly due to the increase of the Curie temperature with pressure itself. For most of the temperature range below T_c the resistivity decreases under pressure, as would be expected due to band broadening.

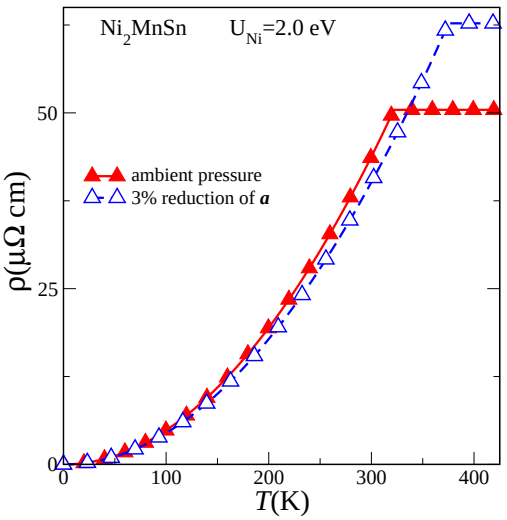

Figure 10: *The temperature dependence of the resistivity of Ni_2MnSn calculated for the ambient pressure and the pressure corresponding to 3% reduction of the lattice parameter.*

Conclusions

We have studied magnetic, thermodynamic, and transport properties of quaternary Heusler alloys $(Ni,Cu)_2MnSn$ by means of the first-principles density functional method. In agreement with experiments, magnetic moments per formula unit depend only weakly on the alloy composition, having values around 4 μ_B.

Exchange interactions were determined using the DLM reference state, which assumes no *a priori* magnetic ordering in the system. The alloy disorder strongly influences values of exchange integrals, resulting in different behaviors of Ni-rich and Cu-rich alloys, which can be ascribed to the 3rd NN exchange integrals. The Curie temperatures, estimated by using the RPA applied to the non-random Mn-sublattice, agree reasonably well with available experimental data.

The residual resistivities are found to obey the weak-scattering Nordheim rule. This is due to the fact that the strong disorder found in $(Ni,Cu)_2MnSn$ alloys influences the states far from the Fermi energy, which are not relevant for electronic transport. Using a simple model for the spin-disorder, we have estimated the temperature-dependent resistivity at temperatures above T_c. Reasonably good agreement with experimental results is found for calculations which assume that the resistivity above T_c is essentially captured by the DLM model. Using this value of resistivity and calculated Curie temperatures, good agreement with the experiment was obtained also for the temperature-dependence of the resistivity below T_c.

Under pressure, the alloy T_c decreases on the Cu-rich side and increases on the Ni-rich side. The variation of T_c can be described by two competing factors: increase in the bare exchange interaction and a decrease of the local moment due to band broadening. The temperature dependent spin-disorder resistivity in Ni_2MnSn at the Curie temperature increases with pressure, but this result is mostly due to the increase of the Curie temperature with pressure itself. For most of the temperature range below T_c the resistivity decreases under pressure, as would be expected due to band broadening.

A systematic study of the magnetic, transport and thermal properties, including their pressure dependence, of similar mixed Heusler alloys involving Fe and Co are currently under way.

Acknowledgment

S.K.B's work was supported by a grant from the Natural Sciences and Engineering Research Council of Canada. J.K. and V.D. acknowledge financial support from AV0Z 10100520 and the Czech Science Foundation (202/09/0775 and 204/11/1228).

References

1. S.K. Bose, J. Kudrnovský, V. Drchal, and I. Turek, Phys. Rev. B **82** (2010) 174402.
2. O.K. Andersen and O. Jepsen, Phys. Rev. Lett. **53** (1984) 2571 .
3. I. Turek, V. Drchal, J. Kudrnovský, M. Šob, and P. Weinberger, *Electronic Structure of Disordered Alloys, Surfaces and Interfaces* (Kluwer, Boston, 1997).
4. S.H. Vosko, L. Wilk, and M. Nusair, Can. J. Phys. **58** (1980) 1200 .
5. E. Uhl, Monatshefte für Chemie **113**, 275 (1982).

6. I. Turek, J. Kudrnovský, V. Drchal, and P. Bruno, Philos. Mag. **86** (2006) 1713.

7. K. Carva, I. Turek, J. Kudrnovský, and O. Bengone, Phys. Rev. B **73** (2006) 144421.

8. I. Turek, J. Kudrnovský, V. Drchal, L. Szunyogh, and P. Weinberger, Phys. Rev. B **65**, 125101 (2002).

9. T. Kasuya, Prog. Theor. Phys. **16** (1956) 58

10. B.L. Gyorffy, A.J. Pindor, J. Staunton, G.M. Stocks, and H. Winter, J. Phys. F: Metal Phys. **15** (1985) 1337.

11. M. Pajda, J. Kudrnovský, I. Turek, V. Drchal, and P. Bruno, Phys. Rev. B **64** (2001) 174402.

12. M.B. Stearns, J. Appl. Phys. **50**, 2060 (1979).

13. S. Isida, H. Asato, E. Iwashima, Y. Kubo, and J. Ishida, J. Phys. F: Metal Phys. **11**, 1035 (1981).

14. E. Uhl, Monatshefte für Chemie **113** (1982) 275.

15. Y. Noda and Y. Ishikawa, Journal of the Phys. Soc. Japan **40**, 690 (1976).

16. G.L. Fraga, J.V. Kunzler, and D.E. Brandao, J. Phys. Chem. Solids **46** (1985) 1071.

17. W.H. Schreiner, D.E. Brandao, F. Ogiba, and J.V. Kunzler, J. Phys. Chem. Solids **43**, 777 (1982).

18. D. Bloch and R. Pauthenet, J. Appl. Phys. **36**, 1229 (1965).

19. Y. Yamamoto, N. Nakagiri, M. Nomura, H. Tange, and H. Fujiwara, Jap. J. Appl. Phys. **18**, 2139 (1979),

20. E. DiMasi, M.C. Aronson, and B.R. Coles, Phys. Rev. B**47**, 14301 (1993).

21. A.G. Gavriliuk, G.N. Stepanov, V.A. Sidorov, and S.M. Irkaev, J. Appl. Phys. **79**, 2609 (1999).

22. I.G. Austin and P.K. Mishra, Philos. Mag. **15**, 529 (1967).